

RICA - Radio Imaging Combination Analyzer

1 MILES LUCAS^{1,2}

2 ¹*Iowa State University, Ames, Iowa*

3 ²*National Radio Astronomy Observatory, Socorro, New Mexico*

4 ABSTRACT

5 1. INTRODUCTION

6 In radio synthesis imaging a common problem arising from interferometry is the lack of zero-spacing
7 data. Without this data, images lack total power information. Single dish radio telescopes retain
8 this total power information but lack the angular resolution capabilities of radio interferometers. To
9 solve this problem, astronomers combine the interferometry data with the total power data. This
10 report seeks to characterize the effectiveness of different combination methods and parameters.

11 The parameters analyzed were multiscale deconvolution versus normal Hogbom deconvolution, the
12 effect of single-dish size on the combination, masking, and number of total iterations (i.e. depth of
13 clean). One of the previous assumptions is that if the single-dish UV-coverage does not adequately
14 complement the interferometer UV-coverage, feathering will not be effective. Another assumption is
15 that simple point structures should not see much discrepancy in parameters or methods. Multiscale
16 deconvolution is supposed to help pick up fluffy structure better due to its multi-pass method of
17 creating model images in the Cotton-Schwab Cycle, as opposed to Hogbom's δ -function method.
18 Therefore, more complex, fluffy structure ought to show more distinction in results.

19 There are four methods of combination that were tested. The first is CASA's *feather* task. The
20 process of feathering starts with regridding the lower resolution to the higher resolution image. Each
21 is then Fourier transformed and gridded, while the lower resolution data is scaled by the ratio of the
22 clean beams (high resolution/low resolution). The high-resolution grid is then added to this, scaled

23 by a weighting that starts at 0 and increases to 1 as the wavelength increases. This final combination
 24 is then inverse Fourier transformed back into the image plane.

25 The next method is using the total power image as the starting model in CASA’s *tclean* task. In
 26 the Cotton-Schwab CLEAN algorithm (CSCLEAN), each major-cycle begins with a blank model
 27 image and constructs an image on it by using minor-cycle iterations. By using a starting model,
 28 this model is no longer blank, but is passed as a parameter. By using the total power image as the
 29 starting model, we can hope to retain the total power information through the CLEAN algorithm.

30 Another modification to the Cotton-Schwab cycle in order to combine images is by doing a modi-
 31 fied joint deconvolution. In each major Cotton-Schwab cycle, the visibilities are gridded and inverse
 32 Fourier transformed to create an image residual, which is then feathered with the total power residual
 33 before deconvolving. The deconvolved model is then convolved with the single-dish beam and sub-
 34 tracted from the previous single-dish residual. The deconvolved model is also Fourier transformed,
 35 degridded, and subtracted from the visibilities to create a new residual image. These residuals are
 36 then degridded and transformed to finish the major cycle. See [Figure 1](#) for a visual flowchart of the
 37 process.

38 The last method of combination we use is *tp2vis*, which takes the total power image and spoofs a
 39 measurement set. The way *tp2vis* accomplishes this is by taking Fourier data from the total power
 40 image and sparsely sampling the Fourier data at close spacings (see [Koda et al. 2011](#)). This data
 41 can be concatenated with the interferometer data and deconvolved in *tclean*. [Figure 2](#) shows how
 42 the single-dish is simulated and concatenated with the interferometer data. This should help fill
 43 the close-spacing gap created by the interferometer data and subsequently help increase total power
 44 information.

45 2. METHODS

46 In order to evaluate the different combination methods, a metric needed to be created and tested
 47 on a suite of models. The metrics used were CLEAN residuals, fidelity images, and a ratio of the
 48 power spectrum densities (PSD). The fidelities are given [Equation 1](#)

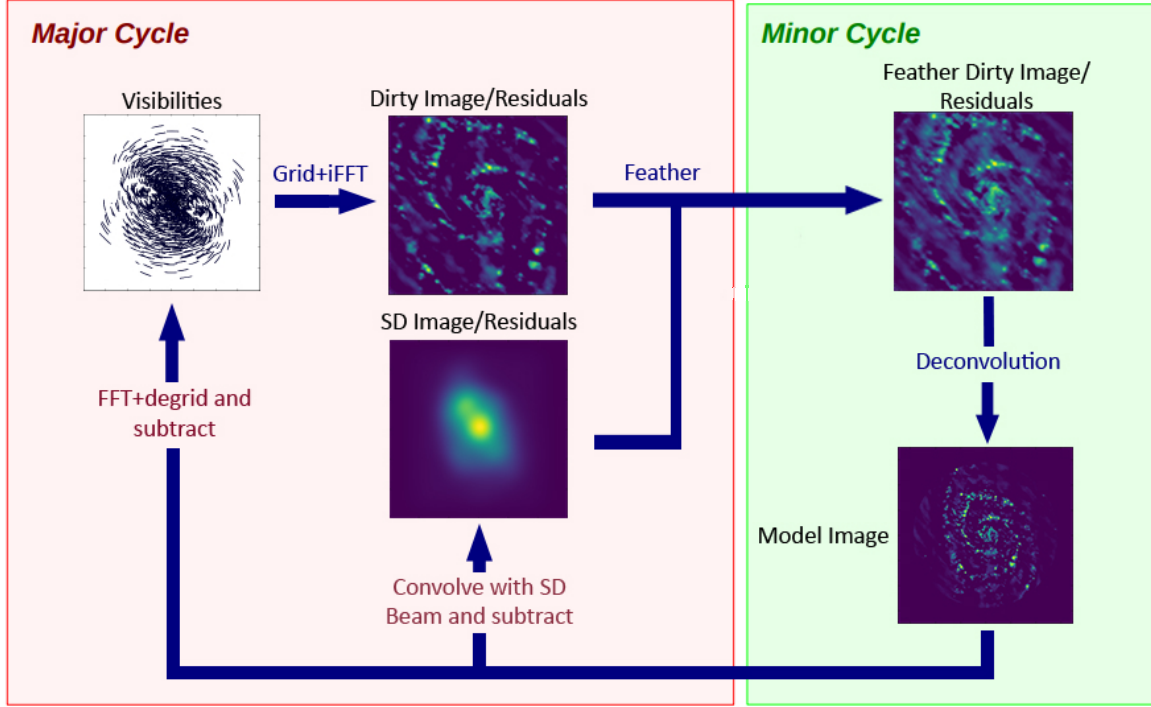


Figure 1. A flow chart describing the joint-deconvolution approach to combining interferometer and single dish data. Adapted from Rau, U. & Naik, N. 2018 (in prep).

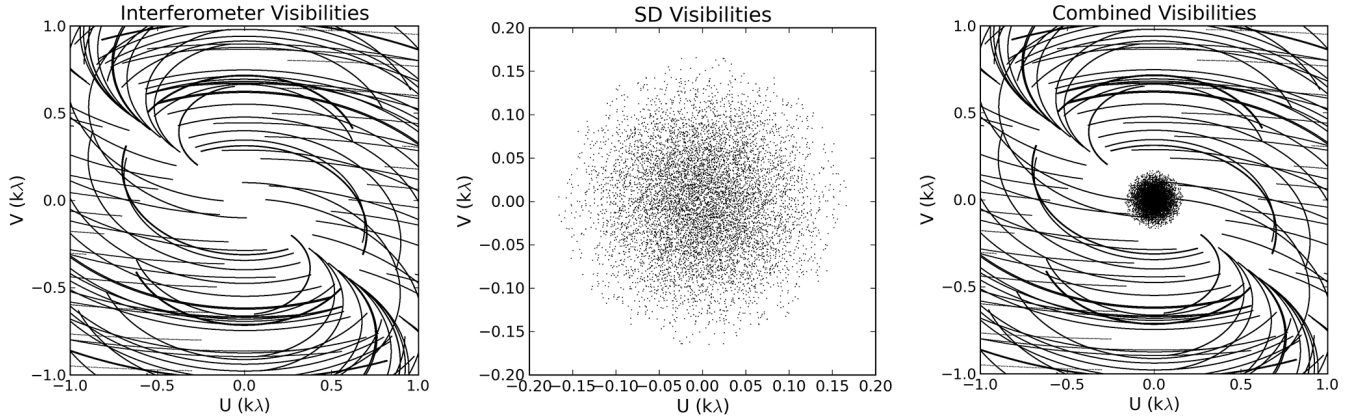


Figure 2. A look at how the visibilities are added through using tp2vis for a model simulated on the VLA A configuration. In the center of the interferometer image in the first plot shows sparsity that is filled in on the third plot. The second plot shows the approximation tp2vis makes of the single dish.

$$\text{Fidelity}(i, j) = \frac{|\text{Model}(i, j)|}{\max(|\text{Difference}(i, j)|, 0.7 \times \text{rms}(\text{Difference}))} \quad (1)$$

49 where model is the reference image and diff is the difference between the test and reference images
 50 (Pety et al. 2011, p.19). The exigence for using PSDs is that the zero-spacing power is readily visible
 51 for every image. By using these ratios, the closer the ratio is to 1.0 at short spacings (when compared
 52 to the true model), the more accurate the combination. In addition, when compared with the total
 53 power image, it shows how much effective weight is given to the total power image in the combination.
 54 The ratio of the PSDs is given by Equation 2

$$\text{Ratio}(UV) = \frac{\text{Power}_{test}(UV)}{\text{Power}_{ref}(UV)} \cdot \frac{\text{BA}_{ref}}{\text{BA}_{test}} \quad (2)$$

$$\text{err}(UV) = \left(\frac{\text{Power}_{ref}(UV) + \text{Power}_{test}(UV)}{2} \right)^{-1} \quad (3)$$

55 where Power is the power from the PSD, BA is the beam area, *ref* refers to the reference image
 56 (model or SD), and *test* refers to whichever image is being tested. The uncertainty given is Equation 3
 57 such that the uncertainty is the reciprocal of the average of the PSDs.

58 Each combination was compared to both the true model and the single dish, total power image.
 59 Many models were tested with various extra parameters. Three models were generated from com-
 60 ponent lists. One has 4 point sources, one has a single Gaussian source, and one has a mixture of 4
 61 point sources, one very broad Gaussian, and one off-center, stronger Gaussian. There were also various
 62 models based off real structure, including M51 (based off an H- α image), Orion, RXJ1347, which is
 63 a source displaying the Sunyaev-Zel'dovich effect (Kitayama et al. 2016), and a protoplanetary disk
 64 (PPD) simulation. Figure 3 shows all of the models. It is important to note that these models have
 65 been regridded onto a common coordinate system that is not representative of the true astronomical
 66 targets. This was an effort to simplify the simulation process for creating measurement sets.

67 The code base for testing the effectiveness is hosted publicly for anyone to use¹. In the source code
 68 there are many scripts and methods to facilitate simulating, combining, and comparing. Every model

¹ <https://gitlab.com/mileslucas/rica>

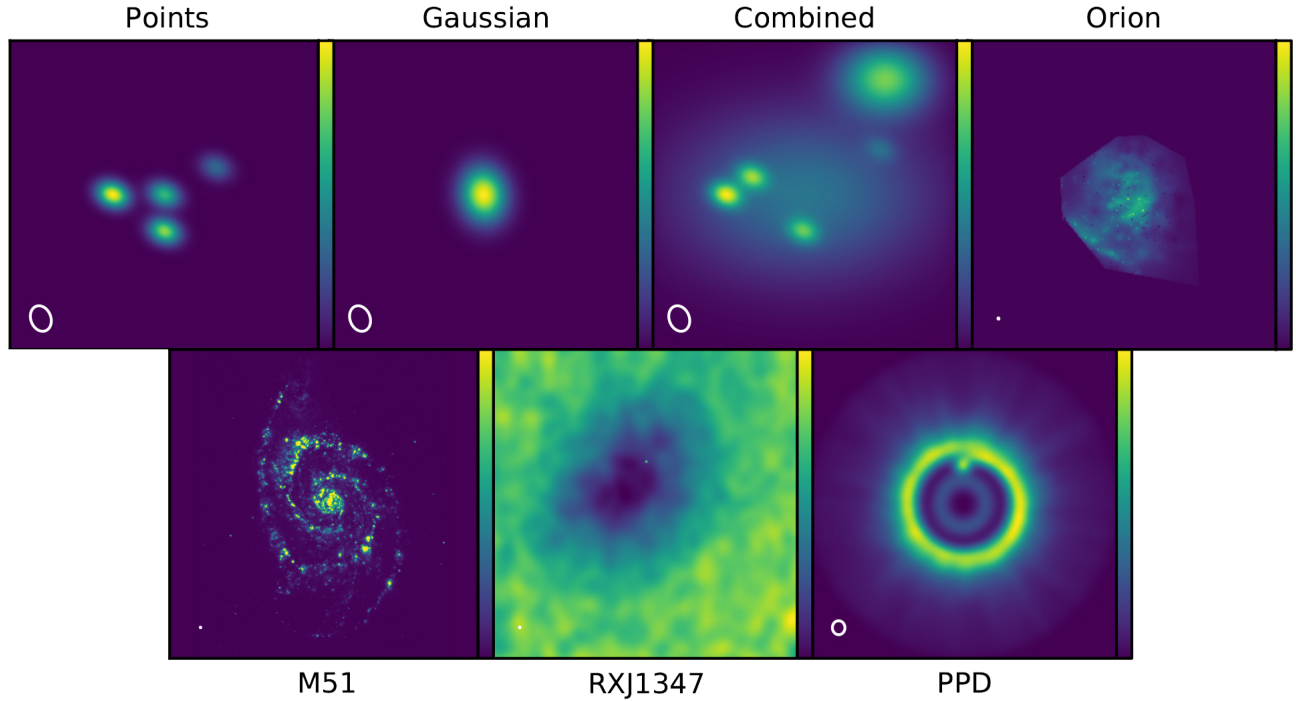


Figure 3. The models used for testing combination methods convolved with some restoring beam to show structure better.

is described in `src/_models.py` with a dictionary defining the simulation and `tclean` parameters. The pipeline for testing these models was as follows:

1. Simulate measurement set (MS) based on VLA configurations
2. Simulate single dish image by convolving model with Gaussian
3. Image the MS
4. Do the combinations (feather, startmodel, joint deconvolution, and `tp2vis`)
5. For each combination, do a comparison with the true model (convolved with the restoring beam) and the single dish image

and is implemented in `src/pipeline.py`.

2.1. Simulations and Deconvolution

79 All simulations were done using the VLA for the telescope model except for the PPD simulation,
 80 which was done using *simalma*. Each test model could define which of the VLA configurations to
 81 use, from A, B, BnA, C, CnB, D, and DnC. The spectral window for the simulations mimic the
 82 VLA C-band at 4.5 GHz to 5.5 GHz (central 5 GHz) with 101 channels at 10 MHz intervals. The
 83 field observed was J2000 21h28m31.0 45°0'0.0''. The observation date and time was 2018/06/01 at
 84 12:00:00.0 UTC. The integration time was 10 s each with a total of 30 000 s. Finally, the data was
 85 corrupted with 1 mJy of simple noise.

86 The PPD model was created by following the [CASA guide for simulation](#). The base model is from
 87 [Wolf & D'Angelo \(2005\)](#), which is a simulation of ALMA data at 672 GHz. This involved one pointing
 88 at J2000 18h00m00.031s -22d59m59.6s observed for 20 min in the ALMA configuration 20. The total
 89 power image was created using *simalma* to recreate the Atacama Compact Array (ACA) with its
 90 12 m single dish telescopes.

91 The single dish images were created by taking the true model and convolving with a Gaussian
 92 equivalent to the single dish beam at the given frequency.

$$\text{FWHM}(\nu, D) = \frac{3.66 \times 10^8 \text{ m s}^{-1}}{\nu \cdot D} \quad (4)$$

93 [Equation 4](#) gives the Gaussian kernel full-width half-maximum (FWHM) in radians for a frequency
 94 in Hz and dish diameter in meters. For instance, to simulate data from the Green Bank Telescope
 95 (GBT) with a dish diameter of 100 m at 5 GHz gives a FWHM of 2'31'', which is in agreeance with
 96 values from the GBT proposer's guide². Note that this is not the most accurate equation for other
 97 telescopes, because there is a constant involved in this equation based off the taper-length of the
 98 telescope's feedhorns. In addition, these single dish images have 5×10^{-6} uniform noise added.

99 Each model defines its own parameters for cleaning. [Appendix A](#) lists every single parameter for
 100 each model. As a default, a model simulated in VLA D configuration has an image size of 64 with
 101 a cell size of 7.0''. The restoring beam for the D configuration is approximately 20.41'' by 15.60'' so
 102 the cell accounts for half to a third of the beam width. In general, cleaning was done with very high

² p.9, <https://science.nrao.edu/facilities/gbt/proposing/GBTpg.pdf>

103 numbers of iterations, relying on a threshold to stop the algorithm for consistency. This differs for
 104 the models tested at explicitly different cleaned levels.

105 **2.2. Comparisons**

106 Each comparison was ran with the same clean parameters for consistency. Because *feather* does
 107 not actively clean, it has its own set of parameters, but all of the models tested used the default
 108 parameters. After all the combination permutations were imaged, they were compared against the
 109 true model convolved with the restoring beam and the single dish image alongside the uncombined
 110 interferometer image. All of the ratio were saved into individual CSV files for further analysis. In
 111 all, each model has 10 comparisons (5 against the models and 5 against the single-dish images) and
 112 4 separate cleans to perform.

113 In order to run a new model to test comparison methods, there are two general methods. If there
 114 exists a true model, simply add an entry to the models dictionary defining the simulation and clean
 115 parameters. It is also important to edit *src/simulate.py* to accommodate the new model. Follow the
 116 existing code base for guidance. It is also important to create a copy of the model and regrid it to
 117 the common coordinate system (use an existing model to retrieve the coordinate system). The model
 118 can then be ran through the pipeline along with any other models using *src/pipeline.py*.

119 If there is no true model, it is still useful to test and compare against the total power image, alone. In
 120 this case, using a cleaned image, a measurement set, and a total power image with the *src/combine.py*
 121 script will produce all of the combinations. These can then be compared using *src/compare.py*. It is
 122 possible to edit *src/pipeline.py* to accommodate special models, see how the PPD model is handled
 123 in the pipeline.

124 **3. RESULTS**

125 For fidelity images and ratios of every comparison, see [Appendix B](#). This section will only comment
 126 on a few models and comparison highlighting trends. The effect of single dish size was apparent on
 127 the accuracy of combinations. [Figure 4](#) shows how the ratios compare between the 100 m single dish
 128 size for the Orion model in B configuration and the 25 m single dish size of the same model. Notably,

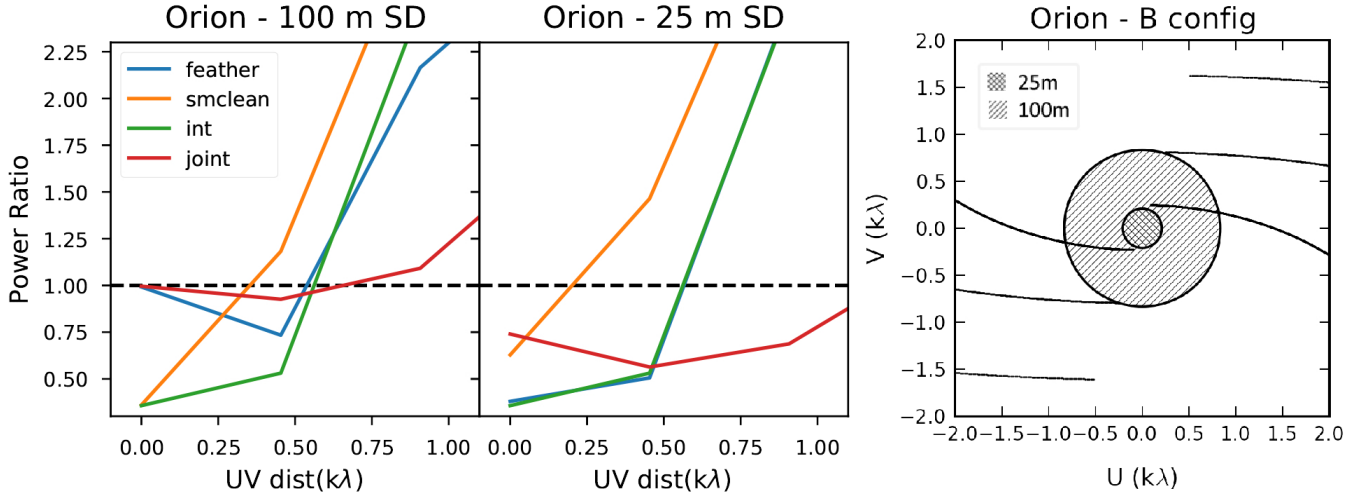


Figure 4. The left two plots are ratios for each combination method between two different single dish sizes. The horizontal line marks the ideal ratio for close UV spacing. The right plot shows the UV coverage of the interferometer with the coverage of the 100 m and 25 m single dishes overlaid.

129 *feather* does not work as well for small single dish sizes. Both start model and joint deconvolution
 130 combination methods are able to do better than the plain interferometer with the small dish, but
 131 still do not reach that ideal ratio that is possible for the larger single dish. Looking at the coverage
 132 of the single dishes, the 25 m dish does not overlap with the interferometer data at all.

133 Next, Figure 5 shows the effect that depth of cleaning has on the power ratios. Each row corre-
 134 sponds to each model and each column is a depth of cleaning based on the number of iterations of
 135 deconvolution. The ‘combined’ model is a much simpler model than the ‘orion-b’ model. First, the
 136 joint deconvolution worked well regardless of the depth of cleaning for both models. Even completely
 137 dirty images had great total power information. After some amount of cleaning, *feather* quickly rose
 138 to the same level as joint deconvolution and in the ‘combined’ model, using a start model started
 139 working after some cleaning. In the simpler, ‘combined’ model, all combination methods converged
 140 at high enough iterations- even the interferometer image. However, for the more complex, ‘orion-b’
 141 model, start model never converged and the values of the ratios remained erratic even at full cleaning
 142 depth.

143 Figure 6 shows how multiscale deconvolution affects the combinations. For each model, there are
 144 some slight variations, but in general the ratios stay consistent. The ‘orion-b-25’ multiscale model

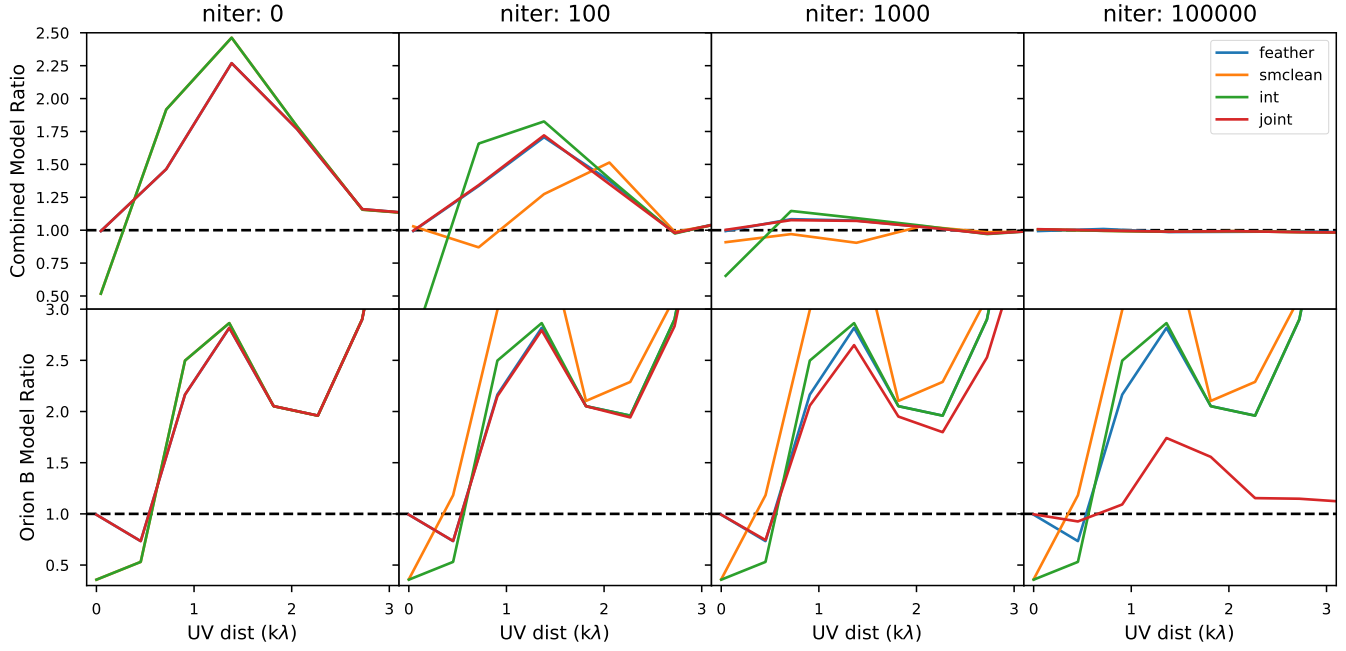


Figure 5. A comparison showing the effect on the combinations due to the depth of cleaning for two models, ‘combined’ and ‘orion-b’. The dashed black line represents the ideal ratio for the true model comparison.

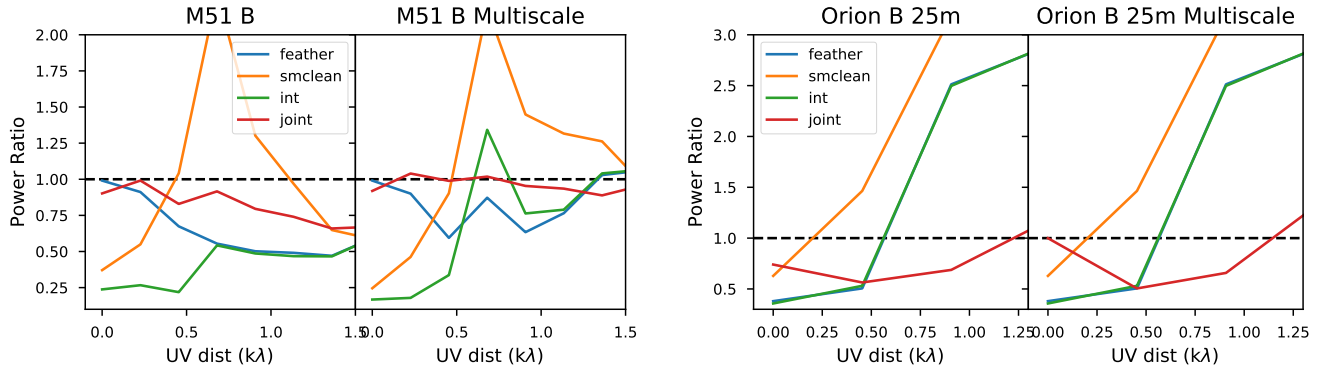


Figure 6. A comparison showing the effect on the combinations due to multiscale deconvolution for two models, ‘m51-b’ and ‘orion-b’. The dashed black line represents the ideal ratio for the true model comparison.

145 shows how multiscale can improve efficiency for joint deconvolution when the single dish overlap is
 146 low. The ‘orion-b’ multiscale model (not shown) does not show much change between deconvolvers
 147 except for an unexplained overshoot in the multiscale joint deconvolution.

148 Figure 7 shows the effect masking has on the combinations. For the simple ‘points’ model masking
 149 causes issues, especially with startmodel. Also, in the ‘orion-b’ model, the startmodel value falls at 0

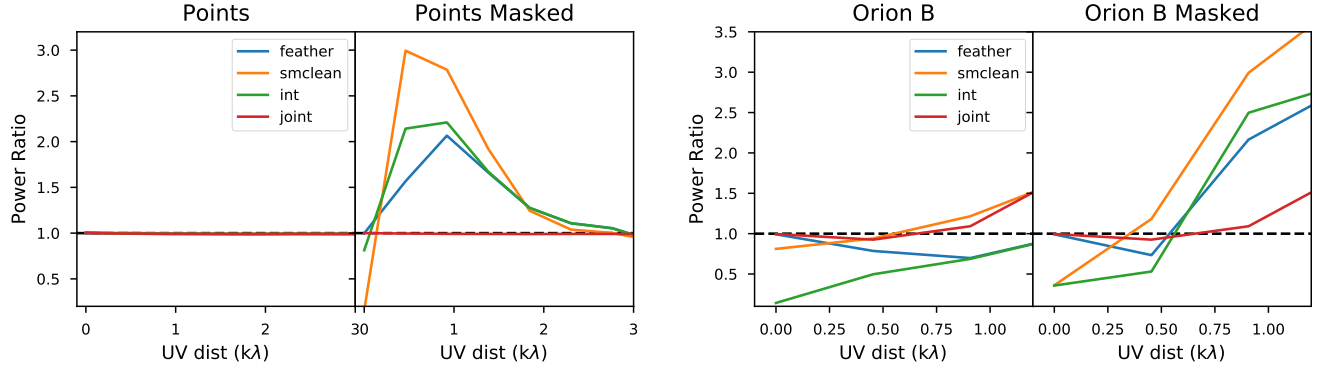


Figure 7. A comparison showing the effect on the combinations due to masking for two models, ‘points’ and ‘orion-b’. The dashed black line represents the ideal ratio for the true model comparison.

UV spacing, as well as the plain, cleaned image. In general, the masking decreases the convergence of the combination methods at the same clean level and may have further affects by changing the performance of the uncombined image. This is also apparent in the ‘RXJ1347’ masked model, where the 0 UV spacing value does not change but the convergence is definitely affected.

Figure 8 shows an overview of the performance of different models. Simpler models with point sources and Gaussians converge at a ratio of 1 and show very little difference until scales at hundredths of a ratio. The more complex models have no easy, clear trend. Each one of these combinations is highly dependent on the structure and parameters. It is interesting that the ALMA ‘PPD’ model only performs well with startmodel and that *feather* and joint deconvolution actually perform worse than the uncombined image.

4. CONCLUSION

From the results of the single dish sizes, the main factor in algorithm success is the amount of overlap of the single dish and interferometer data. This could be the reason why *feather* fails so much and why joint deconvolution and start model are not quite as good, either. Future studies might find the point at which there is enough overlay for each method to “succeed”.

In regards to the depth of cleaning, in general, more is better. Joint deconvolution seemed to work for any dirty image with enough single dish coverage, but for future studies, it would be nice to try and see if joint deconvolution works for dirty images of many more models. In conjunction with the

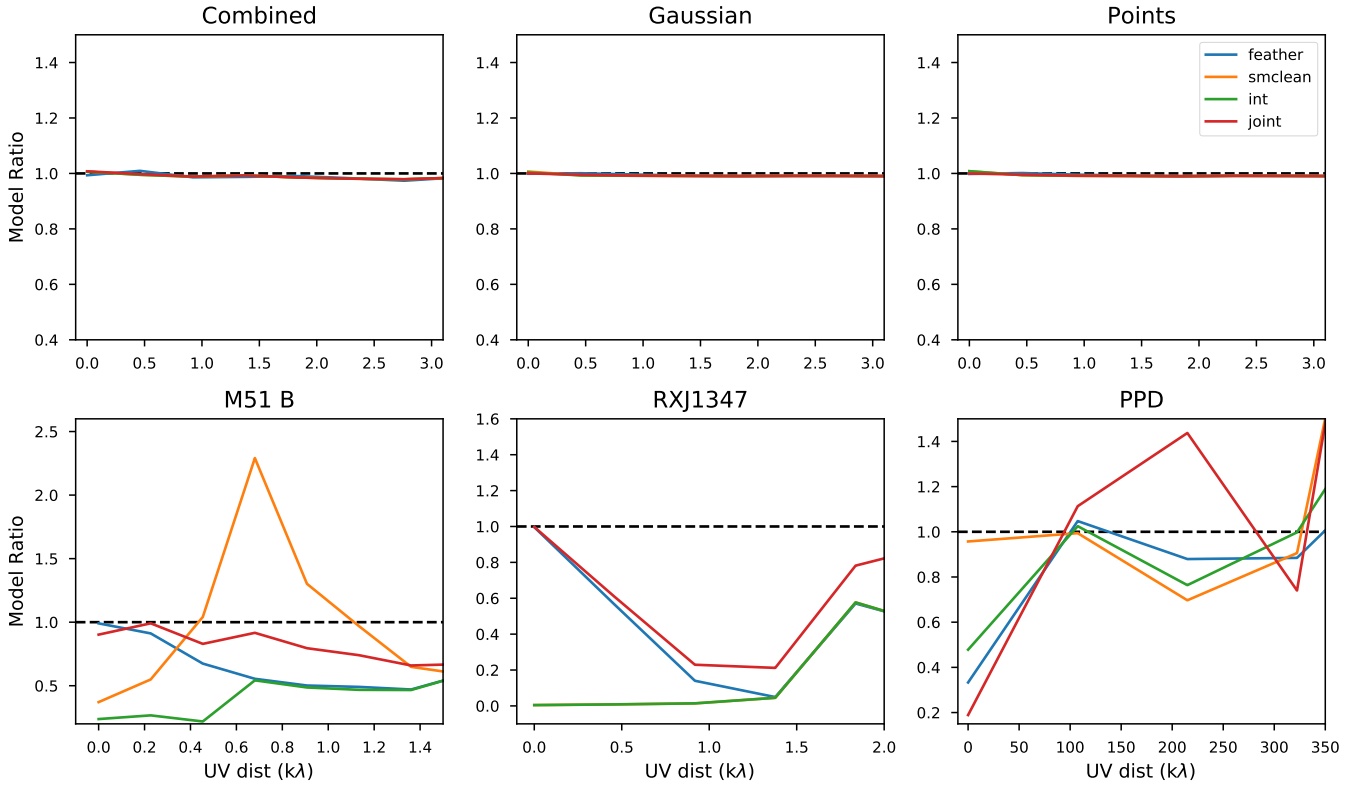


Figure 8. A comparison of many models. The top row are ‘simple’ models that do not contain much structure or extended emission, whereas the second row contains more complex models with different structural scales and interesting phenomenon (Sunyaev-Zel’dovich effect in RXJ1347).

study on single dish size, there were no combinations that retrieved the total power information well from the dirty image due to insufficient single dish coverage³

The multiscale analysis shows that using the multiscale deconvolver can make up for lack of single dish UV coverage in some instances. When there is already decent

Thank you to Dr. Kumar Golap and Dr. Takahiro Tsutsumi for their guidance and assistance. This work was funded by the National Science Foundation in partnership with the National Radio Astronomy Observatory and Associated Universities Incorporated.

³ see ‘orion-b-25-n0’ ratio data

175 *Software:* CASA, tp2vis (Koda et al. 2011)

REFERENCES

- 176 Kitayama, T., Ueda, S., Takakuwa, S., et al. 2016¹⁸¹ Pety, J., Gueth, F., & Guilloteau, S. 2011, ALMA
177 PASJ, 68, 88, doi: [10.1093/pasj/psw082](https://doi.org/10.1093/pasj/psw082) ¹⁸² Memo #398 Impact of ACA on the Wide-Field
178 Koda, J., Sawada, T., Wright, M. C. H., et al. ¹⁸³ Imaging Capabilities of ALMA, Tech. rep.
179 2011, ApJS, 193, 19, ¹⁸⁴ Wolf, S., & D'Angelo, G. 2005, ApJ, 619, 1114,
180 doi: [10.1088/0067-0049/193/1/19](https://doi.org/10.1088/0067-0049/193/1/19) ¹⁸⁵ doi: [10.1086/426662](https://doi.org/10.1086/426662)

186

APPENDIX

187

A. MODEL PARAMETERS

188

189

190

The following table describes the parameters used for cleaning the model images. The only exception is the model ‘combined-sp’, which additionally uses specmode=’cube’ and nchan=-1 to facilitate cube imaging. For more details, look at the *src/_models.py* file, which this table is generated from.

Table 1. The parameters for every model ran through the pipeline

Name	Model	Config	SD size	imsize	cell	niter	cycleniter	threshold	deconvolver	scales	mask
points	points	VLA d	100 m	[64, 64]	7.00arcsec	100000	100	1e-5Jy	hogbom	No	
points-masked	points	VLA d	100 m	[64, 64]	7.00arcsec	100000	100	1e-5Jy	hogbom	Yes	
gauss	gauss	VLA d	100 m	[64, 64]	7.00arcsec	100000	100	1e-5Jy	hogbom	No	
combined	combined	VLA d	100 m	[64, 64]	7.00arcsec	100000	100	1e-5Jy	hogbom	No	
combined-sp	combined	VLA d	100 m	[64, 64]	7.00arcsec	100000	100	1e-5Jy	hogbom	No	
combined-n0	combined	VLA d	100 m	[64, 64]	7.00arcsec	0	100	1e-5Jy	hogbom	No	
combined-n100	combined	VLA d	100 m	[64, 64]	7.00arcsec	100	100	1e-5Jy	hogbom	No	
combined-n1000	combined	VLA d	100 m	[64, 64]	7.00arcsec	1000	100	1e-5Jy	hogbom	No	
combined-ms	combined	VLA d	100 m	[64, 64]	7.00arcsec	100000	100	1e-5Jy	multiscale	[0, 3, 10, 30]	No
m51	m51	VLA d	100 m	[128, 128]	7.00arcsec	100000	100	1e-12Jy	hogbom	No	
m51-ms	m51	VLA d	100 m	[128, 128]	7.00arcsec	100000	100	1e-12Jy	multiscale	[0, 3, 10, 30]	No
m51-b	m51	VLA b	100 m	[1400, 1400]	0.65arcsec	100000	100	1e-12Jy	hogbom	No	
m51-b-ms	m51	VLA b	100 m	[1400, 1400]	0.65arcsec	100000	100	1e-12Jy	multiscale	[0, 3, 10, 30]	No
orion-b-unmasked	orion	VLA b	100 m	[700, 700]	0.65arcsec	100000	400	1e-9Jy	hogbom	No	

Table 1 continued on next page

Table 1 (*continued*)

Name	Model	Config	SD size	imsize	cell	niter	cycleniter	threshold	deconvolver	scales	mask
orion-b	orion	VLA b	100 m	[700, 700]	0.65arcsec	100000	400	1e-9Jy	hogbom	Yes	Yes
orion-b-n0	orion	VLA b	100 m	[700, 700]	0.65arcsec	0	100	1e-9Jy	hogbom	Yes	Yes
orion-b-n100	orion	VLA b	100 m	[700, 700]	0.65arcsec	100	100	1e-9Jy	hogbom	Yes	Yes
orion-b-n1000	orion	VLA b	100 m	[700, 700]	0.65arcsec	1000	100	1e-9Jy	hogbom	Yes	Yes
orion-b-ms	orion	VLA b	100 m	[700, 700]	0.65arcsec	100000	400	1e-9Jy	multiscale	[0, 3, 10, 50]	Yes
orion-b-25	orion	VLA b	25 m	[700, 700]	0.65arcsec	100000	400	1e-9Jy	hogbom	Yes	Yes
orion-b-25-n0	orion	VLA b	25 m	[700, 700]	0.65arcsec	0	100	1e-9Jy	hogbom	Yes	Yes
orion-b-25-n100	orion	VLA b	25 m	[700, 700]	0.65arcsec	100	100	1e-9Jy	hogbom	Yes	Yes
orion-b-25-n1000	orion	VLA b	25 m	[700, 700]	0.65arcsec	1000	100	1e-9Jy	hogbom	Yes	Yes
orion-b-25-ms	orion	VLA b	25 m	[700, 700]	0.65arcsec	100000	400	1e-9Jy	multiscale	[0, 3, 10, 30]	Yes
orion-c	orion	VLA c	100 m	[216, 216]	2.12arcsec	100000	400	1e-9Jy	hogbom	No	No
RXJ1347	RXJ1347	VLA a	100 m	[2268, 2268]	0.20arcsec	100000	100	1e-6Jy	hogbom	No	No
RXJ1347-masked	RXJ1347	VLA a	100 m	[2268, 2268]	0.20arcsec	100000	100	1e-6Jy	hogbom	Yes	Yes
ppd	ppd	ALMA 20	12 m	[192, 192]	0.01arcsec	100000	100	1e-7Jy	hogbom	No	No

191

B. MODEL RESULTS

192 For data tables of every single comparison, visit the [RICA repository](#).

193 **Fig. Set 1. Model Results**

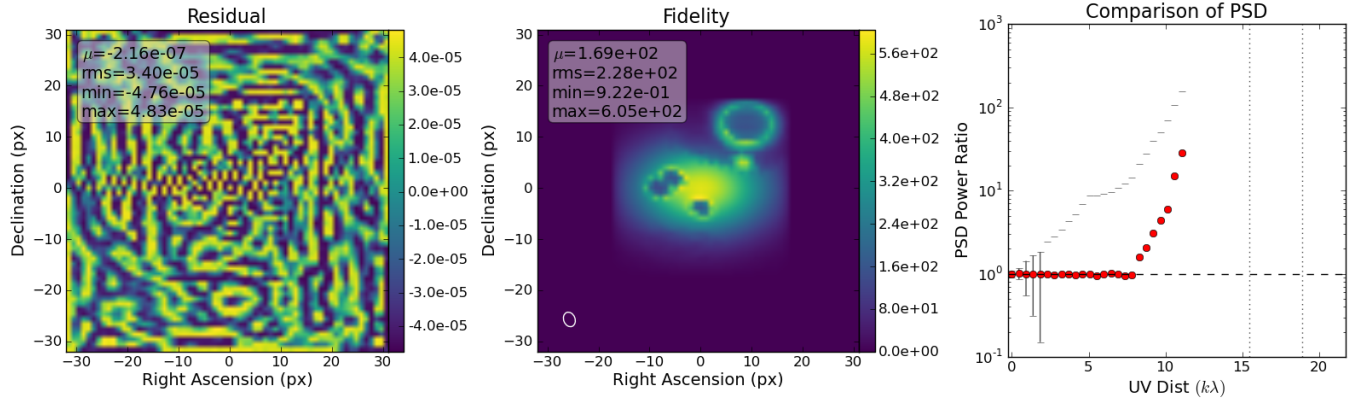


Figure 9. Comparison of feather combination to the true model for combined simulation. The ratio is Equation 2. The black ticks are error bars on a scaled uncertainty based on Equation 3. The vertical lines are the maximum UV distance of the interferometer at the longest and shortest wavelengths, respectively. The complete figure set (125 figures) is available at the [RICA repository](#).